Title
SIMULATION OF PHOTOSYNTHESIS, A RESOURCE FOR ENERGY

Author
Willner, I.

Publication Date
1979-08-01

Lawrence Berkeley Laboratory
UNIVERSITY OF CALIFORNIA

CHEMICAL BIODYNAMICS DIVISION

To be published as a Chapter in U. S.- AUSTRALIA SEMINAR ON BIOELECTROCHEMISTRY, F. Gutmann and H. Keyzer, eds., New York: Plenum Press, 1979

SIMULATION OF PHOTOSYNTHESIS, A RESOURCE FOR ENERGY

Itamar Willner, William E. Ford, John W. Otvos and Melvin Calvin

August 1979

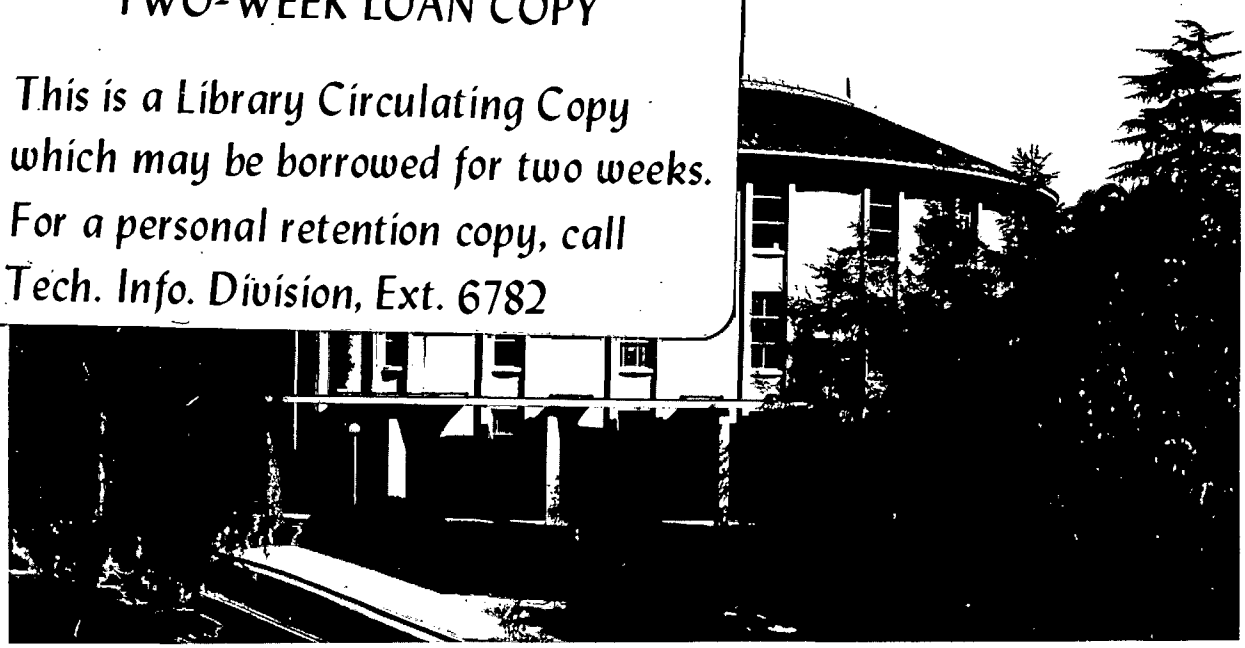

Prepared for the U.S. Department of Energy under Contract W-7405-ENG-48

DISCLAIMER

Simulation of Photosynthesis, A Resource for Energy

Itamar Willner, William E. Ford, John W. Otvos and Melvin Calvin

Lawrence Berkeley Laboratory
Laboratory of Chemical Biodynamics
University of California
Berkeley, California 94720

Abstract

Artificial devices that mimic the photosynthetic pathway are of interest as a fuel source. A basic concept in the design of such devices is the use of dyes to photosensitize electron transfer reactions that produce chemical species capable of oxidizing and reducing water. A fundamental limitation accompanying the photodecomposition of water involves back reactions of the intermediary redox species, whereby the potential energy of the photochemical process is degraded. The introduction of interfaces as kinetic barriers to overcome this limitation is discussed. One type of interface is generated with water-in-oil microemulsions. A photo-induced transfer of electrons and protons from the aqueous phase to the organic phase of a water-in-oil microemulsion is sensitized by the tris(2,2'-bipyridine)Ru(2+) complex. EDTA dissolved in the aqueous compartments is oxidized and dimethylamino-azobenzene dissolved in the continuous oil phase is reduced. The electron transfer process is mediated by benzylnicotinamide, an acceptor located at the interface of the system. The second type of interface discussed is generated with lipid bilayer membrane vesicles. An amphiphilic tris(2,2'-bipyridine)Ru(2+) complex that is incorporated into the walls of phospholipid vesicles photosensitizes the oxidation of EDTA dissolved in the inner aqueous compartments of the vesicle suspension and the reducion of viologens dissolved in the continuous aqueous phase. Intentionally added membrane-bound electron and proton carriers are not required for electron transport across the vesicle walls. Mechanisms for electron transport are considered.

The photoinduced decomposition of water by using suitable redox catalysts needs further development. The reduction of water to produce H_2 is established; however, the complimentary oxidation of water to O_2 is more difficult due to the need for a multistep electron transfer process. A cycle that involves the partial oxidation of water with the concomitant production of H_2 is presented. In this cycle, the oxidation of water is photosensitized by a manganese complex. The possibilities of utilizing the cycle for production of useful chemicals or oxygen in secondary reactions are described.

Devices that mimic the natural photosynthetic pathway are of considerable interest as fuel sources (1-4). The net reaction in the photosynthetic pathway of green plants is the production of carbohydrates and oxygen from water and carbon dioxide using visible light energy (Eq. 1). However, photosynthesis is a complex process of successive and simultaneous events (5-8). Basically, we might divide the process into the photochemical events during which quantum conversion of solar to chemical

$$H_2O + CO_2 \xrightarrow{h\nu} (CH_2O) + O_2 \qquad [1]$$

energy occurs, followed by a series of dark reactions. Although we do not know the fine details of the quantum conversion part, we do know that it involves two photoactive sites: photosystem I and photosystem II (Z-scheme, Figure 1). In photosystem II the excited pigment transfers an electron to a chain of electron traps (including plastoquinone, cytochrome f, etc.), leaving behind an electron "hole." The oxidized species thus formed ultimately oxidizes water to oxygen, presumably through the mediation of a catalyst that accumulates oxidizing equivalents. In turn, in photosystem I, the excited pigment transfers an electron to a second electron trap, while electrons from trap II are supplied to the electron deficient pigment of photosystem I. The electrons trapped in photosystem I are used for successive reduction of ferredoxin and NADP (nicotinamide adenine dinucleotide phosphate) (6-8). The reduced NADP initiates a set of dark reactions, namely the Calvin cycle, in which CO_2 is reduced to carbohydrates (5). Photosystem II represents the net oxidation of water

to molecular oxygen (Eq. 2). In turn, the reducing power introduced into photosystem I coincides with the electrochemical potential of the redox couple H^+/H_2 at pH 7 (the standard electrochemical-reduction potential of ferredoxin is about -0.4 vs. NHE). Hence, from a thermodynamic point of view the achievement of green plants in reducing ferredoxin is equivalent to the production of molecular hydrogen (Eq. 3). Therefore, the primary events of photosynthesis are equivalent in their redox proeprties to decomposition of water with the creation of a potential fuel (hydrogen)(Eq. 4).

$$H_2O \xrightarrow{h\nu} 1/2\ O_2 + 2H^+ + 2\ \bar{e} \qquad [2]$$

$$2H^+ + 2\ \bar{e} \xrightarrow{h\nu} H_2 \qquad [3]$$

$$H_2O \xrightarrow{h\nu} 1/2\ O_2 + H_2 \qquad \Delta G^\circ = 57\ \text{kcal} \qquad [4]$$

We are attempting to design synthetic devices for fuel production that simulate photosynthetic quantum conversion to the extent that water is decomposed, with the advantage (compared to green plants) that energy requirements for other life processes are absent. A basic principle in photosynthesis is photosensitized electron transfer (9). Therefore, the synthetic system (Fig. 2) includes a sensitizer(s) that mimics the function of chlorophyll. The photoexcited sensitizer transfers an electron to an acceptor (A) to yield a reduced species, A^-. The oxidized sensitizer thus formed oxidizes a donor compound (D), while the sensitizer is regenerated. The reduced acceptor (A^-) and oxidized donor (D^+) are selected so that, thermodynamically, they are capable of reducing and oxidizing water to hydrogen and oxygen respectively (eventually by in-

cluding further catalysts or mediating agents) (2-4). In this way the acceptor and donor agents are recycled and all the components of the system, except water, are catalytic. This schematic presentation shows the essential continuous operation of the artificial device whereby an "uphill" reaction generating a "fuel" is driven by visible light.

However, the practical application of this idea suffers from basic limitations due to the thermodynamically favored back reactions between complementary couples formed in the redox cycle (namely, back reactions of A^- with S_{ox} or D^+). Thus, in homogeneous aqueous systems, the "useful" potential energy gain from the formation of the couple A^-/D^+ is degraded. In photosynthesis this fundamental difficulty is solved by natural membranes which function as a barrier for the back reactions. The two "half reactions" that take place in the two photoactive sites are accomplished at opposite sides of a membrane spearating two aqueous compartments. So the oxidation and reduction processes are physically separated and the back reactions are prevented (10,11). Therefore, it seems desirable to adopt the "membrane principle" in the consturction of an artificial device to overcome the intrinsic problem of back reactions.

As one of our objectives in the creation of an artificial photosynthetic unit, we wished to introduce interfaces between two water compartments and conduct a "vectorial" electron transfer across the interfaces (12,13). The principles and characteristics of several electron transfer processes across interfaces and their possible utilization in an artificial photosynthetic device will be the subject of our discussion.

Photoinduced Electron Transfer Across a Water-Oil Interface

Surfactant molecules aggregate to reversed micelles in organic solvents similar to their aggregation to micelles in water. Reversed micelles are capable of dissolving water, thus forming a microemulsion of "water pools" in a continuous oil phase (Fig. 3) (14). The proposed general model for the utilization of microemulsions in the photolysis of water is represented in Fig. 4. The model system is composed of two half-cells that include a microemulsion of water in a continuous organic phase represented as two water droplets. Using two sensitizers, S_1 and S_2, coupled redox reactions are initiated photochemically to produce an oxidized donor (D_1^+) and a reduced acceptor (A_2^-) in the two separate half cells. The complementary redox products of this process (A_1^- and D_2^+) are confined by solubility to the organic phase, so the (favored) back electron-transfers are expected to be inhibited by the introduced interface. The two half cells are bridged by electron and proton carriers (for example a quinone) and thus A_1 and D_2 are regenerated. The reduced and oxidized agents A_2^- and D_1^+ are coupled to the reduction and oxidation of water to regenerate A_2 and D_1. In this way all the components of the system, except water, are recycled.

In order to justify the proposed model for the separation of the complementary products of a redox reaction, we wished to demonstrate electron transfer from a donor in the aqueous phase to an acceptor in the continuous organic phase (12). In principle, the overall electron transfer process can be divided into two distinct parts: (a) from the water to an acceptor located at the interface and (b) from the interphase to an acceptor dissolved in the continuous organic phase. The

electron transfer from the water phase to an acceptor at the interface was investigated in a microemulsion in which the donor, ethylenediamine-N,N,N',N'-tetracetate (EDTA) and sensitizer, tris(2,2'-bipyridine)ruthenium(II)($Ru(bipy)_3^{2+}$) were dissolved in the "water pools." The acceptor used in the system was 1,1'-dihexadecyl-4,4'-bipyridinium chloride (HV^{2+}). This acceptor is expected to be located in the interphase boundary due to its amphiphilic structure. The size of the "water pools" in a water in oil microemulsion is estimated to be 20-30 Å based on light-scattering measurements (15). Hence, the statistical distribution of the sensitizer in the "water pools" ensures many "collisions" with the interface during the lifetime of $*Ru(bipy)_3^{2+}$ ($\sim$ 0.6 μs) (16). A typical preparation of the microemulsion involved the addition of 0.15 ml of 0.3 M $(NH_4)_3$ EDTA aqueous solution (pH = 8.5) and 21 μl of a 0.010 M $[Ru(bipy)_3]Cl_2$ aqueous solution to 2.9 ml of toluene. The acceptor, HV^{2+} (0.9×10^{-3} M) and dodecylammonium propionate (220 mg, 0.3 M relative to the total volume) were added and the mixture was vortex-stirred until clear. The solution was deaerated and illuminated with intervals of continuous blue light (440 nm < λ < 550 nm, incident photon flux $\sim$ 10-16 $\times 10^{-7}$ einstein s^{-1}). The successive formation of the blue hexdecylviologen radical ($HV^{+\cdot}$) was followed spectroscopically by measuring the increase in its absorption at 735 nm (ε = 2500 $M^{-1}cm^{-1}$)(17). The rate of formation of $HV^{+\cdot}$ is displayed in Fig. 5 with two different concentrations of the sensitizer. The maximum quantum yield, ϕ_{max}, based on $HV^{+\cdot}$ formation, was found to be 1.3 $\pm$ 0.4%. Introduction of air into the cuvette reoxidized $HV^{+\cdot}$ to HV^{2+}, and the $Ru(bipy)_3^{2+}$ concentration appeared to be unchanged relative to its initial concentration. As can

be seen from Fig. 5, after three minutes of illumination the concentration of $HV^{+\cdot}$ was 3.6×10^{-4} $M \cdot l^{-1}$. Since the initial concentration of the sensitizer was 7×10^{-5}M, the results reflect that the photosensitizer was recycled during the redox reaction. The results obtained are rationalized by the following redox cycle (Fig. 6). Photoexcited $Ru(bipy)_3^{2+}$ transfer an electron to the interphase-located acceptor HV^{2+}. The resulting $Ru(bipy)_3^{3+}$ oxidizes EDTA and thus the photosensitizer is recycled. These results are consistent with an electron transfer from a donor dissolved in the "water pools" to an acceptor located in the interphase boundary.

However, in order to simulate the general scheme proposed in Fig. 4, electron transfer to an acceptor dissolved in the continuous organic phase is required. The basic idea to achieve this process is displayed in Figure 7. An acceptor (A_1) that is originally located in the interphase region, while its reduced form is extracted into the bulk organic phase, seems to fulfill these requirements. Coupling of the reduced acceptor ($A_1^{[red]}$) with a second acceptor (A_2), soluble in the continuous organic phase, is expected to reoxidize the interface-located acceptor, while reducing A_2. In this way, the net compartmentalization of a reduced acceptor and oxidized donor is accomplished. Benzylnicotinamide (BNA^+) seems to fulfill the central requirement of the interface-located acceptor, since its amphiphilic character instures its initial concentration at the interface, while upon reduction it will be extracted to the bulk organic phase due to charge removal (18). Hence, we have investigated a photosensitized electron transfer using BNA^+(4.8×10^{-3} M) instead of HV^{2+} in a microemulsion in which the composition of the "water pools" was similar to the previous experiment (ammonium EDTA, pH = 8.5, as donor and $Ru(bipy)_3^{2+}$ as sensitizer, bulk concentration 10^{-5} M). In

the organic phase a second acceptor was dissolved, 4-dimethyl-aminoazobenzene (5×10^{-5} M). This acceptor is expected to regenerate the interface-located acceptor while being reduced (19). Since 4-dimethyl-aminoazobenzene absorbs in the visible spectrum (λ = 402, ε = 22000 $M^{-1}cm^{-1}$), while the hydrazo derivative is colorless, its reduction can be followed spectroscopically, and a probe for the electron transfer process is established. Illumination of this microemulsion in a dearated cuvette with intervals of blue light yields a successive reduction of the dye and disappearance of its absorption at λ = 402 nm. The changes in the dye concentration as a function of illumination time are represented in Fig. 8. After four minutes of illumination, 80% of the dye had been reduced ($\phi_{max} = 0.13 \pm 0.04\%$). The product of the dye reduction was identified as the corresponding hydrazo derivative because introduction of oxidizing agents such as I_2 or H_2O_2 resulted in regeneration of 4-dimethylaminoazobenzene. At the end of the photoreduction, the sensitizer concentration appeared to be unchanged. The quantitative reduction of the dye, in comparison to the experimental mole ratio of dye: $Ru(bipy)_3^{2+}$ (5:1), indicates that the sensitizer was recycled during the photoinduced redox reaction. Control experiments revealed that all the components in the system were crucial to the reduction of the dye. By excluding $Ru(bipy)_3^{2+}$, EDTA or BNA^+, the photoinduced reduction of the dye was prevented. The fact that BNA^+ was required in the process emphasizes that it served as a mediating agent in the cycle. The results are explained by a cyclic redox mechanism presented in Fig. 9. The electron transfer from photoexcited $Ru(bipy)_3^{2+}$ to BNA^+ is followed by the reduction of the dye dissolved in the continuous organic phase.

The oxidized photosensitizer is reduced by EDTA, while the initial sensitizer is regenerated. The net oxidation-reduction reaction accomplished by visible light sensitization is the reduction of 4-dimethylaminoazobenzene by EDTA. Based on the known oxidation products of EDTA (20,21), the accomplished process is summarized in Eq. 5. To estimate the thermodynamic balance of this reaction, we used glycine as a model for the oxidation site of EDTA and found that the reaction is uphill in free energy ($\Delta G^\circ \sim 37$ kcal/mole of EDTA consumed):

$$R_1\text{-}N(CH_2CO_2^-)(CH_2CO_2^-) + R_2\text{-}N{=}N\text{-}R_3 + 2H_2O \rightarrow R_1\text{-}NH\text{-}CH_2CO_2^- + CH_2O + HCO_3^- + R_2\text{-}NH\text{-}NH\text{-}R_3 \quad [5]$$

Since BNA^+ serves as a model for NADP, the redox reaction accomplished in the microemulsion system may be visualized as a biomimetic approach to photosystem I, in which NADP is reduced. The photoinduced reduction of 4-dimethylaminoazobenzene demonstrates that an electron transfer across the interface of a water-oil microemulsion has been carried out along an endoergic pathway. The system therefore represents a model for the compartmentalization of a redox reaction.

Photosensitized Electron Transport Across Lipid Vesicle Walls

Pigmented membranes that are asymmetric with respect to electron donating and accepting species in the separate aqueous phases could, in principle, be used to convert solar energy to chemical form by mediating photosensitized electron transfer reactions vectorially across the membrane. By coupling the redox reactions to oxidation and reduction of water, the decomposition of water could be achieved. The redox chemistry of photoexcited dyes usually involves one-electron transfers, while

multielectron transfers are required to produce molecular hydrogen or oxygen from water, so the accumulation of charges is required. One of the functions of the membrane would be as a barrier to diffusional recombination of reactive intermediates accumulated in the aqueous compartments.

Membrane-mediated electron transfer between aqueous compartments requires charge transport through two phase boundaries as well as through the membrane interior, so high specific interfacial area and thinness are two related properties that are desirable. Suspensions of lipid bilayer vesicles are practically optimal with regard to these properties. The composition of vesicles can be varied conveniently. The ordered, liquid crystalline nature of vesicles could prove important for efficient energy and electron transfer among their components. These are some of the reasons that we have been exploring the possibility of using vesicles as substrates for photosensitized decomposition of water.

Photosensitized electron transport across lipid bilayer membranes is a relatively new field of research (22-27). Although the ability of lipid layers to transmit electrons is established, the mechanism and conditions for electron transport are not certain. Several fundamental questions need to be addressed, particularly whether electrons can be transmitted across the membrane directly between pigment molecules, or whether electron carriers that diffuse across the membrane, or provide a transport chain, are required. We should also keep in mind that electron transport through the membrane needs to be coupled to proton transport in the same direction (or some other means of maintaining charge neutrality).

As a model for studying photosensitized charge transport across vesicle walls, we have used a membrane-bound tris(2,2'-bipyridyl) ruthenium(2+) derivative with two n-hexadecyl substituents (abbreviated to Ru^{2+}; see Fig. 10) to mediate transfer of electrons from EDTA, dissolved in the encapsulated aqueous compartments of egg yolk phosphatidylcholine (PC) vesicles, to viologens dissolved in the continuous aqueous phase of the vesicle suspension (13).

Besides PC and Ru^{2+}, initially we included in the vesicle walls hexadecylviologen ($C_{16}V^{2+}$), vitamin K_1 quinone, and decachlorocarborane to assist charge transport across the membrane-water interface and membrane interior, in case they were needed. MV^{2+} was dissolved in the continuous aqueous phase. The vesicles were prepared in EDTA solution (as its ammonium salt) (pH 7) by the injection technique (28), followed by gel filtration to replace the external EDTA solution with ammonium acetate solution containing MV^{2+} and Zn^{2+}. We observed the production of $MV^{+\cdot}$ upon illumination of the vesicle system with intervals of continuous visible light (Fig. 11c; $\phi_{max} \sim 5 \times 10^{-5}$). The appearance of $MV^{+\cdot}$, measured spectrophotometrically, had a sigmoidal dependence on the total amount of light absorbed by Ru^{2+}, with saturation after about 10% of the MV^{2+} had been reduced. However, EDTA oxidation is irreversible and this reaction proceeds in homogeneous solutions photosensitized by $Ru(bipy)_3^{2+}$ (Fig. 11a) (29), so control experiments were required to insure that we were observing photosensitized electron transport <u>across</u> the vesicle walls. EDTA that was not removed by gel filtration, or that might have "escaped" from the vesicle interiors, was rendered inactive by adding an excess of zinc ions to the vesicles after gel filtration. The effect of Zn^{2+} on the reaction is shown in Fig. 11b for the homogeneous case, and in Fig. 11d after the vesicles had been disrupted by detergent. It

is unlikely that the PC, or ethanol or dimethylformamide used in the vesicle preparation and not removed by gel filtration, was the source of electrons for MV^{2+} reduction because no viologen radical was observed with vesicles containing acetate instead of EDTA ($\phi < 5 \times 10^{-6}$). Finally, the vesicles were found to be practically impermeable to MV^{2+} on the time scale of our experiment (fractional decrease in concentration = 0.04 $\pm$ 0.04 in two hours for escape of 0.20 M MV^{2+} from vesicle interiors).

Our next step was to determine which of the membrane components, besides PC and Ru^{2+}, were required. We found that increasing the pH to 8.5 increased the quantum yield by around seven-fold in the homogeneous case and around five-fold in the vesicle system. Inhibition by zinc ions and stability of Ru^{2+} to hydrolysis of the amide linkages were apparently unaffected by raising the pH, so this change was made. Removal of both vitamin K_1 quinone and decachlorocarborane had little effect, while further removal of hexadecylviologen caused a six-fold decrease in quantum yield (see Table 1). In all cases the cumulative amount of viologen radical produced had a sigmoid dependence on the cumulative illumination time, although the prominence of the induction period varied. The quantum yield for $MV^{+\cdot}$ production had a linear dependence on light intensity when the vesicle walls were composed of PC, Ru^{2+}, and HV^{2+}. When the walls contained just PC and Ru^{2+} and we used heptylviologen (C_7V^{2+}), the water-soluble C-7 analogue of MV^{2+}, instead of MV^{2+} the absolute quantum yield was $(3.8 \pm 0.7) \times 10^{-4}$ (Table 1).

The last system mentioned is the least ambiguous case for considering possible mechanisms for electron transport across the vesicle walls, so we have examined this system in more detail (30). The vesicle composition is shown in Fig. 12. We expect that Ru^{2+} is distributed on both

sides of the lipid bilayer, and oriented so that the charged chromophore is near the vesicle-water interface. The fact that the chromophore of Ru^{2+} is in an aqueous environment in the vesicles is reflected by its uv-vis absorption spectrum, which is sensitive to solvent (unpublished observations). We used for our analysis the kinetic scheme shown in Fig. 13, which is based on the assumption that the primary photochemical event is oxidative quenching of the sensitizing excited state of Ru^{2+} ($*Ru^{2+}$) by C_7V^{2+} rather than a reductive quenching by EDTA, as is the case in homogeneous solutions (29). In the kinetic scheme the vertical lines represent the inner (EDTA side) and outer (C_7V^{2+} side) vesicle surfaces. The five states, labeled A to E, can be considered to interconvert with the first-order rate constants k_0 to k_4. The constancy of the k's implies that the concentrations of the reaction partners on either side of the vesicle wall do not vary significantly. Values for these rate constants consistent with the conditions of our experiments are included; their derivation will be briefly described below. The processes envisaged are as follows: $*Ru^{2+}$ is assumed to be produced with nearly unit quantum yield (A → B), as is the case for $Ru(bipy)_3^{2+}$ (31). $*Ru^{2+}$ decays to the ground state (B → A) or is oxidatively quenched by C_7V^{2+} (B → C). Back transfer of electrons from $C_7V^{+\cdot}$ to Ru^{3+} (C → A) competes with electron transport across the membrane (C → D), which is assumed to be reversible (D → C). Oxidation of EDTA by Ru^{3+} (D → E) is irreversible because of fragmentation and addition of water (21).

We have considered two possible transmembrane electron transport mechanisms: i) there is net diffusion of Ru^{3+} to the EDTA side of the

membrane and Ru^{2+} to the C_7V^{2+} side, and ii) Ru^{2+} on the EDTA side transfers an electron to Ru^{3+} on the C_7V^{2+} side (electron exchange). It is possible to distinguish between these mechanisms in two ways. One way is to compare the rate constant for electron transport across the membrane, k_3, to rate constants for transmembrane diffusion ("flipping") of amphiphilic molecules in phospholipid vesicles (32,33). The two mechanisms also differ in their predicted dependence on the concentration of Ru^{2+} in the vesicle wall (i.e., the mole ratio of PC to Ru^{2+}). Since diffusion is a first-order process, k_3 will be independent of Ru^{2+} concentration. On the other hand, electron exchange is a bimolecular process involving Ru^{2+}, so in this case k_3 will be dependent on Ru^{2+} concentration. The quantum yield we measure for $C_7V^{+\cdot}$ production can be related to k_3 using the kinetic scheme, so the two mechanisms can be distinguished by the quantum yield dependence on the PC to Ru^{2+} ratio.

With the steady-state approximation that the concentrations of $*Ru^{2+}$ and Ru^{3+} are very small, and the assumption that k_3 equals k_{-3}, the overall quantum yield (for sequence $\underline{A} \rightarrow \underline{E}$) is given by:

$$\phi_{AE} = \phi_{AC} \cdot \phi_{CE} = \frac{k_1}{k_0 + k_1} \cdot \frac{k_3 k_4}{k_3 k_2 + k_2 k_4 + k_3 k_4} \qquad [6]$$

where ϕ_{AC} and ϕ_{CE} are the yields for sequences $\underline{A} \rightarrow \underline{C}$ and $\underline{C} \rightarrow \underline{E}$. Now we consider the ratio of quantum yields ϕ'_{AE}/ϕ_{AE} for two experiments with different PC:Ru^{2+} mole ratios, that is, with different concentrations of Ru^{2+} in the vesicle walls. If the diffusional mechanism is operative, then k_3 equals the diffusional rate constant, and

$$\frac{\phi'_{AE}}{\phi_{AE}} = 1.$$

If the transport mechanism is by electron exchange, then

$$k_3 = k_{exch}[Ru^{2+}], \qquad [7]$$

where k_{exch} is the exchange rate constant, so the ratio of quantum yields (R) equals the ratio of Ru^{2+} concentrations (r) times a fraction:

$$R = \frac{\phi'_{AE}}{\phi_{AE}} = r \cdot \frac{1}{1 + (r - 1)\phi_{CE}[1 + \frac{k_2}{k_4}]}, \quad r = \frac{[Ru^{2+}]'}{[Ru^{2+}]} > 1 \qquad [8]$$

We tested the quantum yield dependence for $C_7V^{+\cdot}$ production on Ru^{2+} concentration for two samples; the results are shown in Fig. 14. Both samples contained the same amount of PC, and the PC:Ru^{2+} mole ratios were 200:28 and 200:10. We observed that by increasing the concentration of Ru^{2+} by the factor $r = 2.8 \pm 0.2$, the maximum quantum yield increased by the factor $R = 2.2 \pm 0.3$. Thus our results are consistent with Eq. 8 when the fraction is 0.79 ± 0.16 (estimated uncertainty).

We have described the derivation of an order-of-magnitude estimate for k_3 (30). In summary, the expression for ϕ_{CE} in Eq. 6 was rearranged and solved for k_3 in terms of ϕ_{CE}, k_2, and k_4. ϕ_{CE} was estimated from luminescence quenching data and the measured overall quantum yield ϕ_{AE}. The first order rate constant k_2 was estimated from a literature value for the bimolecular rate constant for reaction between $Ru(bipy)_3^{3+}$ and $MV^{+\cdot}$ (34), and our estimate for the local concentration of $C_7V^{+\cdot}$, that is, at the vesicle surface. Similarly we estimated k_4 (35). Our best estimate for k_3 is about 1×10^5 s^{-1}, but within limits of uncertainty, k_3 varies from 10^3 to 10^6 s^{-1}. Although the uncertainties are large, it is clear that values for k_3 consistent with our results are several

orders of magnitude greater than rate constants for diffusion of amphiphilic molecules across the walls of PC vesicles: $\sim 10^{-6}$ s^{-1} for PC (32), $\sim 10^{-3}$ s^{-1} for cholesterol (36), and $\lesssim 1$ s^{-1} for fatty acids (33). Thus both the rate constant for electron transport across the vesicle walls, and the quantum yield dependence on Ru^{2+} concentration, are inconsistent with a mechanism that depends on "flipping" of the ruthenium complex, whereas the dependence on Ru^{2+} concentration is consistent with an electron exchange mechanism. Our estimate for the rate constant for electron exchange (Eq. 7) between Ru^{3+} and Ru^{2+} in opposing monolayers of the vesicle wall is 10^6 $M^{-1}s^{-1}$, since $k_3 \sim 10^5$ s^{-1} and $[Ru^{2+}] \sim 0.1$ M. For comparison, the exchange rate constant of the $Ru(bipy)_3^{2+}$ + $Ru(bipy)_3^{3+}$ couple is 2×10^9 $M^{-1}s^{-1}$ in acidic aqueous solution (37).

We conclude that our results add support to evidence (22-27) that pigmented lipid bilayer membranes can transmit electrons. Also, it is apparent that diffusional electron-transporting molecules are not required for photosensitized electron transport across vesicle walls. We have interpreted the results in terms of electron eschange between Ru^{2+} and Ru^{3+} complexes at opposing vesicle-water interfaces. The facility with which tris-2,2'-bipyridyl metal ion complexes undergo electron exchange (35) is important in this model. Since the membrane thickness is about three or four times the diameter of the Ru^{2+} chromophore, the exchanged electrons may have to tunnel (22, 24, 38, 39) through part of the hydrocarbon-like core of the membrane. On the other hand, bilayer membranes might be viewed as semiconductors (22, 23).

The model presented assumes that the physical properties of the

vesicles are not significantly different when PC:Ru^{2+} mole ratios are 200:10 and 200:28. However, two properties that could differ are membrane fluidity and degree of lateral phase separation, both a result of chemical differences between PC and Ru^{2+}. Fluidity could affect the average distance between ruthenium chromophores in opposing monolayers, thereby affecting the probability for electron exchange. Lateral phase separation (33), favored by increasing compositional heterogeneity, could cause the appearance of Ru^{2+} aggregates, which is predicted (40, 25) to make electron transport across the membrane more probable. Although we do not expect either effect to play an important role in the present case, further investigation will be required to determine the actual charge transport mechanism, and its dependence on membrane parameters.

Irrespective of the charge transport mechanism, it appears that the rate constant for electron transport across pigmented vesicle walls can be great enough to compete with energy wasting recombination reactions between primary products at the vesicle surface. We find this result encouraging toward our goal of using bilayer membranes in practical solar energy converting devices. We expect that significant improvements can be made in quantum yield by increasing the probability of electron transfer across the membrane (e.g., by increasing the pigment concentration) or decreasing the probability of the recombination reactions (e.g., by taking advantage of surface potentials at charged interfaces) (41,42). With appropriate catalysts for oxygen and hydrogen evolution, the products of photosensitized charge separation can be coupled to decomposition of water. One approach we have in mind utilizes two types of pigmented vesicles in separate half-cells, one type for hydrogen production and the other for oxygen production, with the two

half-cells connected electrochemically (see Fig. 15).

The Utilization of Interfaces in Photodecomposition of Water

The water-in-oil microemulsion and vesicle systems seem to meet the basic need for an artificial membrane that compartmentalizes two redox reactions. However, in order to construct a practical artificial system, one needs to design catalysts for the decomposition of water (Fig. 2). Catalysts for the reduction of water to hydrogen were developed in recent years (43,36). Viologen radicals have an adequate reduction potential to reduce water at acidic pH ($E° MV^{2+}/MV^{+}\cdot$] = -0.44 V). Indeed, it was reported that viologen radicals reduce water in the presence of heterogeneous catalysts like Pt or PtO_2(43,35). Similarly, it has been reported that a Rh complex and colloidal Pt act as mediators in photosensitized reduction of water to hydrogen (44). Recently, a homogeneous Co^{II}-complex was reported to mediate the production of hydrogen by $Ru(bipy)_3^{2+}$ photosensitization (46). Meanwhile, the complementary oxidation reaction accompanying the production of hydrogen involved different donor substrates like EDTA or other tertiary amines, or ascorbic acid (43-46). However, in order to construct a practical fuel device the donor should be an abundant and cheap source viz. water. Indeed, it seems that our main efforts at present should be directed toward the development of catalysts capable of photooxidizing water. The difficulties we envision in the oxidation process of water are presented in Eq. 2. In order to produce one molecule of oxygen, the accumulation of four electrons is required. Thus, the catalyst should exhibit a charge storage capability or it should be possible to perform a concerted four-electron oxidation (47).

Very recently it was reported that $Ru(bipy)_3^{3+}$ generated photochemically oxidzes water to O_2 in the presence of RuO_2 as heterogeneous catalyst (48,49). In these experiments, irreversible acceptors like $[Co^{I}(NH_3)_5Cl]^{2+}$ or Tl^{3+} were utilized. The next steps should involve the coupling of oxygen and hydrogen production in one continuous system. We believe that the interfaces presented in our discussion could play an important role in achieving the required compartmentalization of the oxidation and reduction processes necessary for prevention of competing back reactions. The introduction of solid catalysts into vesicles and "water pool" of microemulsions might be solved by supporting the catalysts on water-soluble polymers (50). In general, however, it seems that the development of homogeneous catalysts for the photodecomposition of water would be advantageous.

In natural photosynthesis, the mechanism of oxygen production is not known. However, it is known that Mn-ions play an important role in oxygen evolution (47). This basic knowledge led Calvin to propose Mn-complexes as catalysts for the oxidation of water in an artificial photosynthetic device (51). This idea (Fig. 16) involves the successive photoinduced oxidation of a Mn^{II}-complex to Mn^{IV}- complex. A stepwise oxidation of water by the Mn^{IV}-complex might occur, and the intermediary peroxy radicals recombine. Ultimately, further oxidation of the peroxy bridge leads to oxygen production and regeneration of the sensitizer. The electrons abstracted during the formation of the Mn^{IV}-complex are used to produce the hydrogen (fuel). Calvin extended the oxygen evolution idea by suggesting a "manganese dimer" as a potential catalyst to carry out a concerted four-electron oxidation of water (3, 52). In the dimeric structure, the combination of two oxygen atoms to liberate oxygen should

be facilitated.

Meanwhile, the utilization of Mn-complexes for the direct evolution of oxygen has been unsuccessful in our hands (53). However, Porter and coworkers reported in 1978 the photoinduced reduction of quinones by a Mn^{III}-porphyrin and the presumably low yield formation of oxygen was suggested (54). The obstacles observed in oxygen evolution by a homogeneous catalyst led us to reconsider the cycle presented in Fig. 16. We speculated that the dimerization process involved in oxygen production scheme is the barrier for the process. So, we attempted to sort out the essential idea presented in Fig. 16, that a Mn^{IV}-complex oxidizes water in a two-electron oxidation process. Thus an Mn^{II}-oxo-complex as an active oxygen transfer agent might be formed. Such oxo-porphyrin complexes of diverse metallo porphyrins are well known (55-57). The "active oxygen" in these complexes is of electrophilic-oxenoid character, and it might be trapped by different nucleophiles or "electron rich" bonds (57). So, instead of using the evolution of molecular oxygen as the "concept" for the water oxidation half-cell, we thought that the production of a Mn^{II}-oxo-complex in the redox cycle might even be advantageous. The basic idea involves the addition of a trapping agent (S_T) that will trap the active oxygen and regenerate the sensitizer (Eq. 9). The "oxygenated" substrate thus produced allows us to accumulate the fuel (hydrogen) during the reduction process that accompanies the formation of Mn^{IV}-complex. In turn, the oxygenated trap, in a secondary process, should be able to produce useful chemicals (A-O) or eliminate oxygen in the presence of additional catalysts (Eqs. 10 and 11). Thus we are no longer restricted to catalysts that will perform concerted four-electron oxidations, and hydrogen production can be separated from

oxygen production (58).

$$Mn{=}O + S_T \rightarrow Mn^{II} + S_T{=}O \quad [9]$$

$$S_T{=}O + A \rightarrow S_T + A{-}O \quad [10]$$

or $$2S_T{=}O \xrightarrow{Cat} 2S_T + O_2 \quad [11]$$

With these guidelines in mind, we have recently succeeded in achieving a photoinduced oxidation of water whereby an active oxygen transfer to triphenylphosphine is accomplished (58). Using a Mn^{III}-porphyrin ($Pn\text{-}Mn^{III}$) as photosensitizer, methylviologen (MV^{2+}) as acceptor, and triphenylphosphine as the active oxygen trap, a redox reaction could be induced by illumination with visible light. The reduction of MV^{2+} and accumulation of the oxygenated trap, triphenylphosphine oxide, while recycling the sensitizer has been accomplished (Fig. 17). Thus, the basic approach by which the photodecomposition of water through an active oxygen transfer was achieved. The development of trapping agents whose oxygenated products are capable of evolving oxygen in the presence of other catalysts, or are themselves useful chemicals, are now under current investigation in our laboratory.

Will water and sunlight be our fuel source in the future? At the moment, it is a philosophical question. We are in the right scientific direction in our separation of the complex natural photosynthetic process and in our attempt to construct artificial devices for its essential parts. The progress in recent years is indeed encouraging. Combining the different parts into one comprehensive system will be the challenge of the future. The fact that nature achieved it gives us a hope that mankind will overcome the problems as well.

Acknowledgement: This work was supported by the Division of Chemical Sciences, Office of Basic Energy Sciences of the U. S. Department of Energy under contract W-7405-ENG-48. Dr. Itamar Willner wishes to thank the Weizmann Institute of Science for a Chaim Weizmann Postdoctoral Fellowship.

Table 1

Effectof vesicle composition on quantum yield of viologen radical production[a]

Additional membrane components	Viologen (1 mM) in continuous aqueous phase	Maximum quantum yield
HV^{2+} (0.01 mM) KQ (0.1 mM) B (0.01 mM)	MV^{2+}	$(2.6 \pm 0.8) \times 10^{-4}$ [b]
HV^{2+} (0.01 mM)	MV^{2+}	$(3.3 \pm 1.0) \times 10^{-4}$ [b,c]
none	MV^{2+}	$(5 \pm 2) \times 10^{-5}$ [b]
none	C_7V^{2+}	$(3.8 \pm 0.7) \times 10^{-4}$ [c]

[a] Vesicle dispersions contained 2 mM PC and 0.1 mM Ru^{2+}; concentrations are bulk values; pH = 8.5; KQ = vitamin K_1 quinone, B = decachlorocarborane

[b] 420 nm < λ < 600 nm illumination

[c] 440 nm < λ < 550 nm illumination

Figure Captions

Figure 1. Electron transfer (Z-scheme) in photosynthesis.

Figure 2. General scheme for water photodecomposition. S represents an artificial sensitizer which simulates the function of the natural chlorophyll.

Figure 3. The formation of water-in-oil microemulsion using reversed micelles.

Figure 4. General scheme for water photodecomposition using two half cells of water-in-toluene microemulsions. The two water droplets represent two kinds of water-in-oil microemulsion.

Figure 5. The photoreduction of hexadecylviologen (HV^{2+}) to the respective radical-cation ($HV^{+\cdot}$) in a water-in-oil microemulsion using ammonium EDTA (0.3 M, pH = 8.5) as aqueous phase and HV^{2+} (0.9×10^{-3} M) as acceptor. (a) $[Ru(bipy)_3^{2+}] = 7 \times 10^{-5}$M (b) $[Ru(bipy)_3^{2+}] = 4 \times 10^{-5}$M. The amount of $HV^{+\cdot}$ is determined by the increase of absorption at 735 nm ($\varepsilon = 2500\ M^{-1}cm^{-1}$).

Figure 6. Electron transfer from the aqueous phase to an acceptor located in the interphase.

Figure 7. The separation of a reduced acceptor and oxidized donor mediated by an acceptor located at the interface.

Figure 8. The reduction of 4-dimethylaminoazobenzene as a function of illumination time, monitored by the decrease of dye absorption at $\lambda = 402$ nm ($\varepsilon = 22000\ M^{-1}cm^{-1}$).

Figure 9. Cyclic mechanism for photoinduced electron transfer across the interface of a water-in-oil microemulsion.

Figure 10. Structural formula for (N,N'-di(hexadecyl)-2,2'-bipyridine-4,4'-dicarboximide)-bis(2,2'-bipyridine)ruthenium(II)$^{2+}$, abbreviated to Ru^{2+} in the text.

Figure 11. Photosensitized reduction of methylviologen in aqueous media using EDTA as electron donor, and inhibition of the reaction by zinc ions: a) Homogeneous conditions using $Ru(bipy)_3^{2+}$ as sensitizer. $[Ru(bipy)_3^{2+}] = 5 \times 10^{-5}$ M, $[MV^{2+}] = 5 \times 10^{-4}$ M, [EDTA] = 1 x 10^{-3} M, ammonium acetate buffer, 1 M, pH = 7. b) Composition as in a) but with 2 x 10^{-3} M zinc acetate added. c) Vesicle dispersion with the amphiphilic analogue of $Ru(bipy)_3^{2+}$, Ru^{2+}, dissolved in the vesicle walls. EDTA is dissolved in the enclosed aqueous compartments and MV^{2+} and Zn^{2+} are dissolved in the continuous aqueous phase. $[PC]_{bulk} = 2 \times 10^{-3}$ M, $[Ru^{2+}]_{bulk} = 1 \times 10^{-4}$ M, $[EDTA]_{inside} = 0.5$ M, $[MV^{2+}]_{outside} = 1 \times 10^{-3}$ M, $[Zn^{2+}]_{outside} = 0.01$ M. Both aqueous phases contained ammonium acetate buffer, pH = 7. d) Composition as in c), but with detergent added (0.018 M of 3-(dimethylhexadecylammonio)-propane-1-sulfonate) to solubilize the vesicles and release the encapsulated EDTA solution. Illumination: 900 watt Xenon arc lamp, 420 nm < λ < 600 nm.

Figure 12. Schematic of bilayer vesicle cross-section, illustrating the composition of the aqueous phases and vesicle wall for 200:10 ($PC:Ru^{2+}$) mole ratio vesicles. The composition of the membrane phase calculated for vesicles of $\sim$ 250 Å outer diameter.

Figure 13. Photosensitized production of heptylviologen radical as a function of cumulative number of absorbed photons for two vesicle compositions: PC:Ru^{2+} mole ratios of 200:10 (O) and 200:28 (□). PC concentration (2 mM) is the same in both samples. Illumination with blue light (440 nm < λ < 550 nm); incident photon intensity = (5.8 ± 0.8) x 10^{-5} einstein min^{-1}.

Figure 14. Kinetic model for photosensitized electron transport across vesicle wall, with estimated first-order rate constants. Vertical lines represent membrane-water interfaces. RH· stands for EDTA less one hydrogen atom.

Figure 15. Scheme for photosensitized decomposition of water using two types of pigmented colloidal particles. In this case the particles are lipid bilayer vesicles. The sensitizing dyes, S_1 and S_2, and catalysts for oxidation and reduction of water, C_1 and C_2, are dissolved in the vesicle walls or in the encapsulated aqueous compartments. The vesicles are immobilized in semipermeable hydrogel beads supported in columns through which aqueous solutions of reversible electron acceptor, A, and electron donor, D, are passed. Reduction of A and oxidation of D take place at the vesicle surfaces during light-driven reactions that are coupled to oxidation and reduction of water. The O_2 and H_2 half-cells are connected electrochemically with two electrodes and a salt bridge. The quantum requirement is eight photons per O_2 molecule produced. The net reactions are:

$$2H_2O + 4A + 4h\nu \rightarrow O_2 + 4H^+ + 4A^-$$
$$4A^- \rightarrow 4A + 4e^- \text{ (electrode)}$$
} O_2 half cell

$$4H^+ + 4D + 4h\nu \rightarrow 2H_2 + 4D^+$$
$$4D^+ + 4e^- \text{ (electrode)} \rightarrow 4D$$
} H_2 half cell

Figure 16. Scheme for photooxidation of water to oxygen using Mn-complexes.

Figure 17. Photoproduction of active oxygen using Mn^{III}-porphyrin as sensitizer. The electron acceptor in the redox cycle is methylviologen (MV^{2+}) and triphenylphosphine serves as the trapping agent.

References

1. V. Balzani, L. Maggi, M. F. Manfrin, F. Bolleta and M. Gleria, Science 189, 852 (1975).
2. J. R. Bolton, Science 202, 705 (1978).
3. M. Calvin, Acc. Chem. Res. 11, 369 (1978).
4. a) G. Porter, Pure and Appl. Chem. 50, 263 (1978).
   b) Photosynthesis in Relation to Model Systems, J. Barber Ed., (Elsevier North-Holland, Inc.: New York, 1979).
   c) M. Calvin, Photochem. Photobiol. 23, 425 (1976).
5. M. Calvin and J. A. Bassham, The Path of Carbon in Photosynthesis (Prentice-Hall: Englewood Cliffs, New Jersey, 1957).
6. D. O. Hall and K. K. Rao, Photosynthesis (Edward Arnold: London, 1972).
7. K. Sauer, Acc. Chem. Res. 11, 257 (1978).
8. a) R. H. Holm, Acc. Chem. Res. 10, 427 (1977).
   b) D. I. Arnon, Proc. Nat. Acad. Sci. 68, 2883 (1971).
9. a) G. R. Seely, Photochem. Photobiol. 27, 639 (1978).
   b) T. J. Meyer, Israel J. Chem. 15, 200 (1977).
10. M. Calvin, J. Theoret. Biol. 1, 258 (1961).
11. M. Gibbs, Ed. Structure and Functions of Chloroplasts (Springer-Verlag: Berlin, 1971).
12. I. Willner, W. E. Ford, J. W. Otvos, and M. Calvin, Nature (London), in press (1979).
13. W. E. Ford, J. W. Otvos, and M. Calvin, Nature (London) 274, 507 (1978).
14. J. H. Fendler and F. J. Fendler, Catalysis in Micelles and Macromolecular Systems (Academic Press: New York, 1975).
15. Y. Y. Lim and J. H. Fendler, J. Amer. Chem. Soc. 100, 7490 (1978).

16. J. Van Houten and R. J. Watts, J. Amer. Chem. Soc. 98, 4853 (1976).

17. E. Steckhan and T. Kuwana, Ber. Bunsenges. 78, 253 (1974).

18. K. Nakamura, A. Ohno, S. Yasui and S. Oka, Tetrahedron Letters, 4 ?5 (1978).

19. B. T. Newbold, "Chapter 15" in The Chemistry of the Hydrazo, Azo, and Azoxy Groups, S. Patai, Ed. (John Wiley & Sons: New York, 1975).

20. V. Massey, M. Stankovich and P. Hemmerich, Biochemistry 17, 1 (1978).

21. A. I. Krasna, Photochem. Photobiol. 29, 267 (1979).

22. D. S. Berns, Photochem. Photobiol. 24, 117 (1976).

23. H. T. Tien in ref. 46, pp. 116-173.

24. H. Kuhn, J. Photochem. 10, 111 (1979).

25. M. Mangel, Biochem. Biophys. Acta 430, 459 (1976).

26. a) K. Kurihara, M. Sukigara, and Y. Toyoshima, Biochim. Biophys. Acta 547, 117 (1979).

b) K. Kurihara, Y. Toyoshima, and M. Sugara, Biochem. Biophys. Res. Commun. 88, 320 (1979).

27. Y. Sudo and F. Toda, Nature 279, 808 (1979).

28. S. Batzri and E. D. Korn, Biochem. Biophys. Acta 298, 1015 (1973).

29. K. Takuma, M. Kajiwara, and T. Matsuo, Chem. Lett., 1199 (1977).

30. W. E. Ford, J. W. Otvos, and M. Calvin, Proc. Nat. Acad. Sci, in press.

31. F. Bolletta, M. Maestri, and V. Balzani, J. Phys. Chem. 80, 2499 (1976).

32. J. E. Rothman and J. Lenard, Science 195, 743 (1977).

33. E. Sackmann, Ber. Bunsenges. Phys. Chem. 82, 891 (1978).

34. J. Kiwi and M. Grätzel, Helv. Chim. Acta 61, 2720 (1978).

35. N. Sutin, J. Photochem. 10, 19 (1979).

36. J. M. Backer and E. A. Dawidowicz, Biochem. Biophys. Acta 551, 260 (1979).

37. R. C. Young, F. R. Keene, and T. J. Meyer, J. Am. Chem. Soc. 99, 2468 (1977).

38. D. Mauzerall in The Porphyrins, Vol. V, Ed. D. Dolphin (Academic Press: New York, 1978), pp. 29-52.

39. V. I. Goldanskii, Nature 279, 109 (1979).

40. A. Illani and D. S. Berns, Biophysik 9, 209 (1973).

41. S. A. Alkaitis, G. Beck, and M. Grätzel, J. Am. Chem. Soc. 97, 5723 (1975).

42. a) C. Wolff and M. Grätzel, Chem. Phys. Lett. 52, 542 (1977).
b) Y. Tsutsui, K. Takuma, T. Nishijima, and T. Matsuo, Chem. Lett., 617 (1979).

43. A. Moradpour, E. Amouyal, P. Keller, and H. Kagan, Nouv. J. Chim. 2, 547 (1978).

44. a) J. M. Lehn and J. P. Sauvage, Nouv. J. Chim. 1, 449 (1977).
b).M. Kirch, J. M. Lehn and J. P. Sauvage, Helv. Chim. Acta 62, 1345 (1979).

45. K. Kalyanasundarum, J. Kiwi and M. Grätzel, Helv. Chim. Acta. 61, 2720 (1978).

46. J. Barber, Ed., Topics in Photosynthesis--Photosynthesis in Relation to Model Systems, Vol. 3 (Elsevier/North-Holland, Biomedical Press: Amsterdam, 1979).

47. A. Harriman and J. Barber in ref. 46, pp. 243-280.

48. J. M. Lehn, J. P. Sauvage and R. Ziessel, Nouv. J. Chim. 3, 423 (1979).

49. a) J. Kiwi and M. Grätzel, submitted for publication, personal communication.

b) K. Kalyanasundaram and M. Gratzel, submitted for publication, personal communication.

50. a) L. D. Rampino and F. F. Nord, J. Amer. Chem. Soc. 63, 2745 (1941).

b) H. Hirai, Y. Nakao, N. Toshima, and K. Adachi, Chem. Lett., 905 (1976).

c) J. Kiwi and M. Gratzel, submitted for publication, personal communication.

51. M. Calvin, Science 184, 375 (1974).

52. M. Calvin, Energy Research 3, 73 (1979).

53. S. R. Cooper and M. Calvin, Science 185, 376 (1974).

54. a) G. Porter, Proc. R. Soc. Lond. A 362, 281 (1978).

b) I. A. Duncan, A. Harriman and G. Porter, J. Chem. Soc., Faraday Transactions II, 1920 (1978).

55. M. Baccouche, J. Ernst, J. H. Fuhrhop, R. Schlozer, and H. Arzoumanian, J. Chem. Soc. Chem. Commun.,821 (1977).

56. J. T. Groves, T. E. Nemo, R. S. Myers, J. Amer. Chem. Soc. 101, 1032 (1979).

57. a) C. K. Chang and M. S. Kuo, J. Amer. Chem. Soc. 101, 3413 (1979).

b) K. B. Sharpless and T. C. Flood, J. Amer. Chem. Soc. 93, 2316 (1971).

58. I. Willner, J. W. Otvos, W. E. Ford, and M. Calvin, submitted for publication.

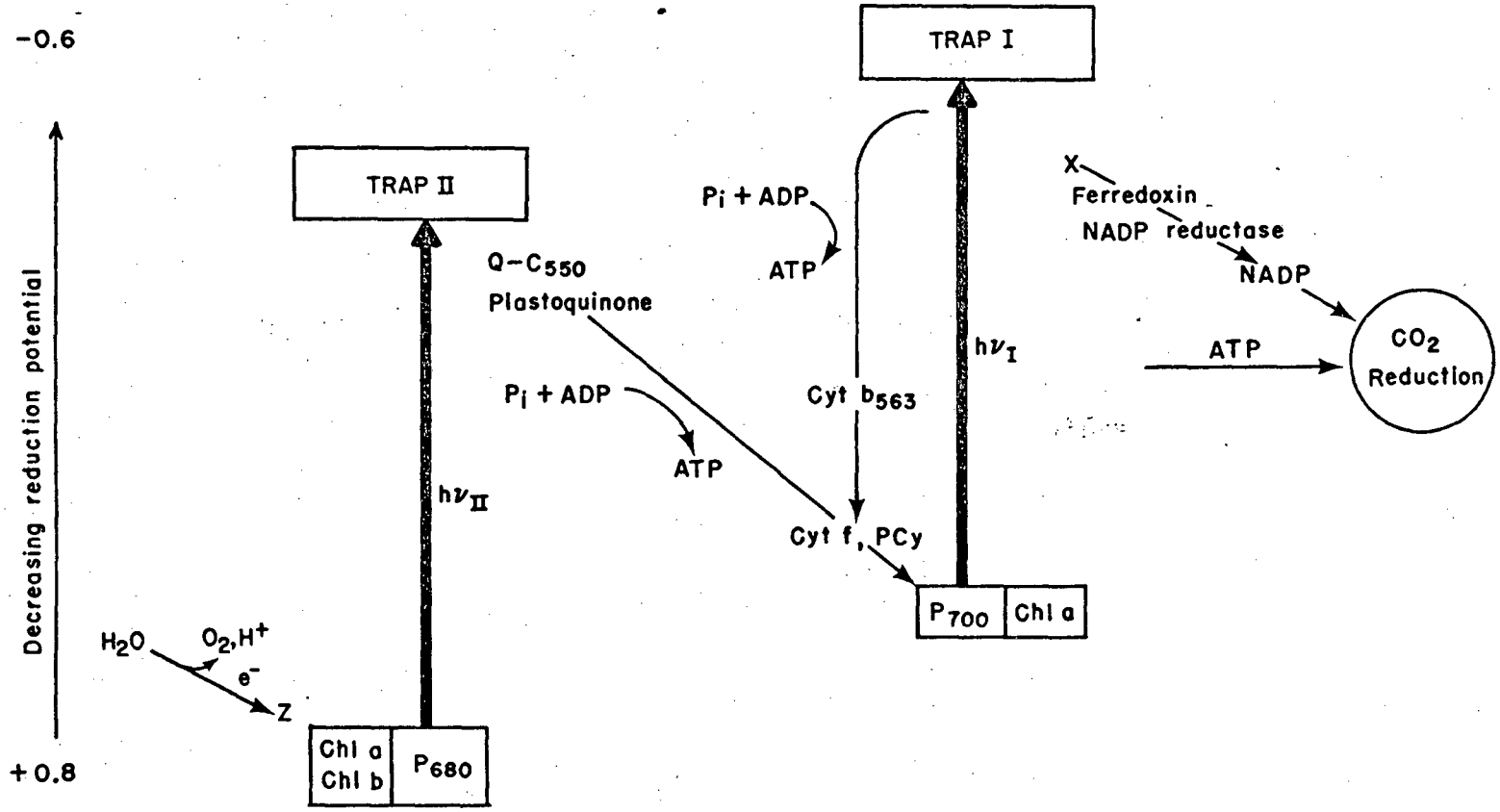

XBL7410-5395 B

Figure 1

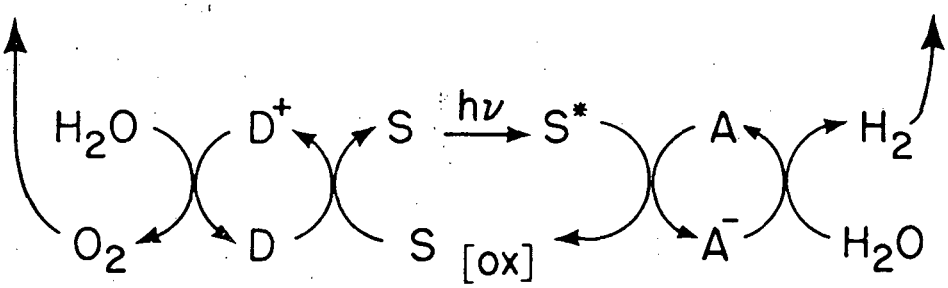

XBL791-4633

Figure 2

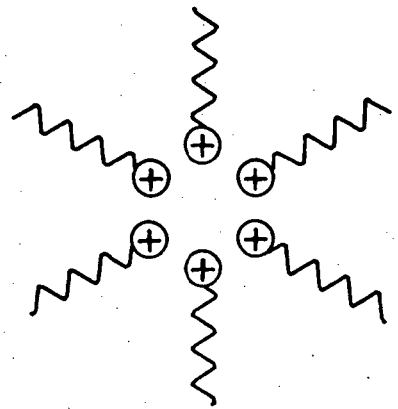

Reverse micelle

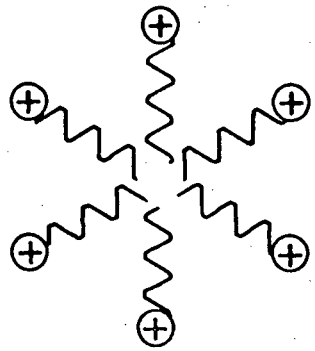

Micelle

Surfactant monomer

XBL798-4980

Figure 3

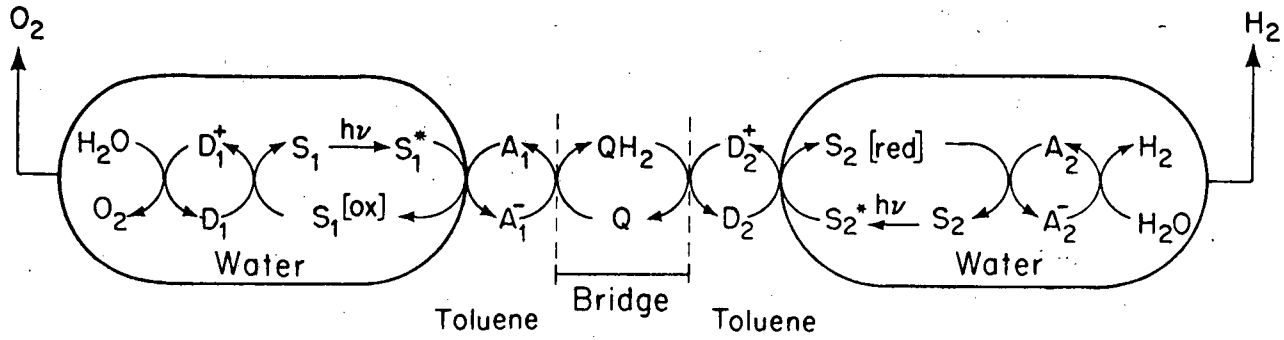

XBL 798-11024

Figure 4

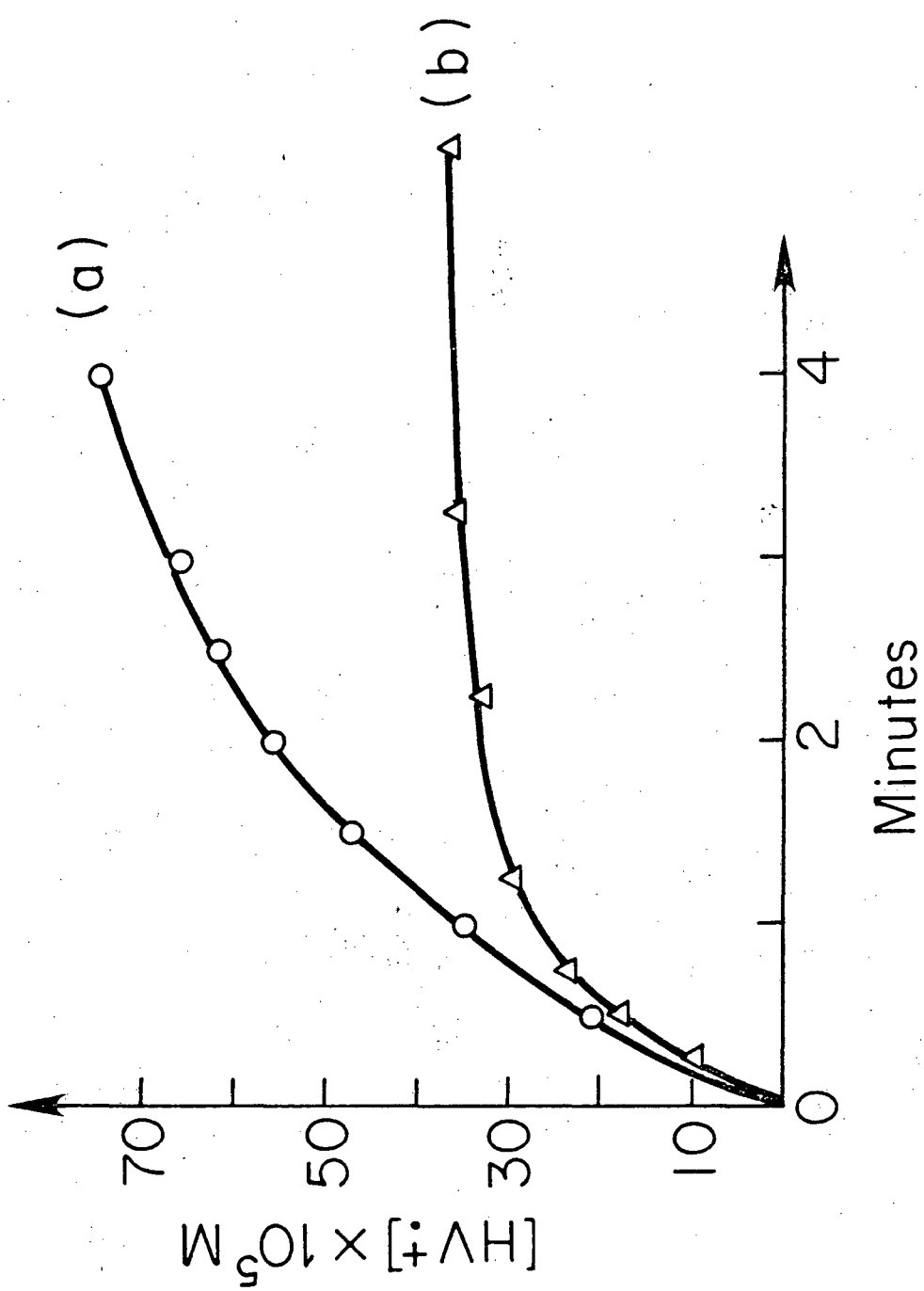

XBL 798-4981

Figure 5

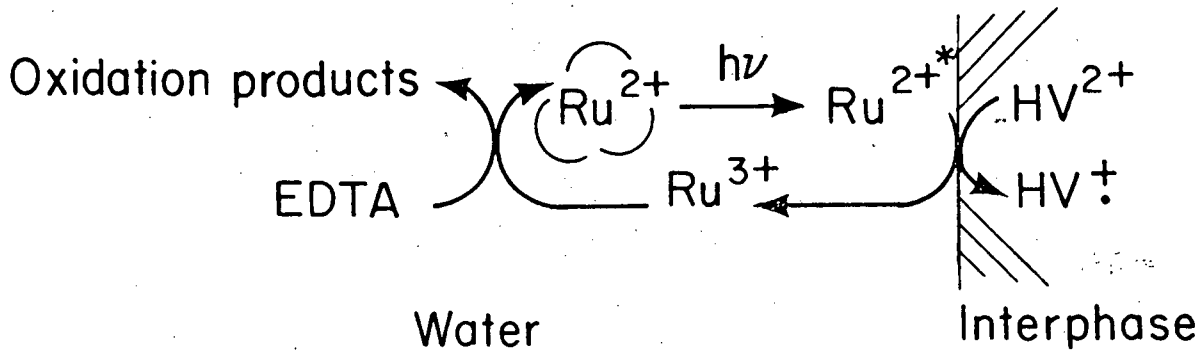

XBL798-4978

Figure 6

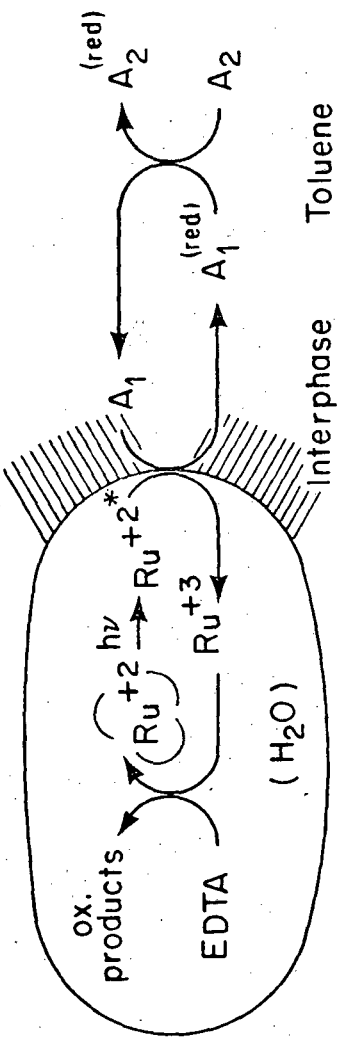
(red)
A2
A2
(red)
A1
A1
Toluene
Interphase
Ru+2*
hν
Ru+2
Ru+3
(H2O)
ox.
products
EDTA

Figure 7

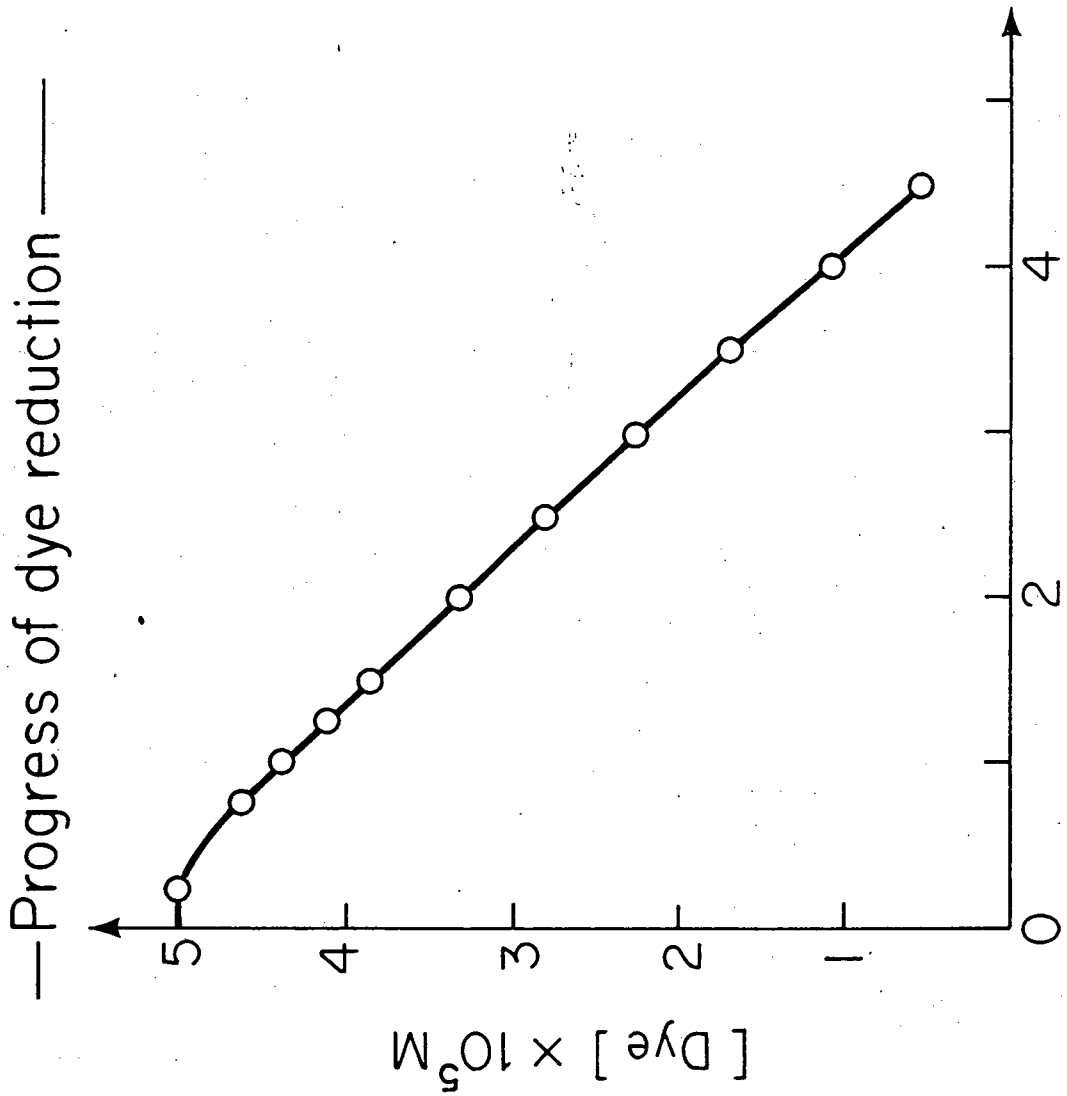

XBL791-4642

Figure 8

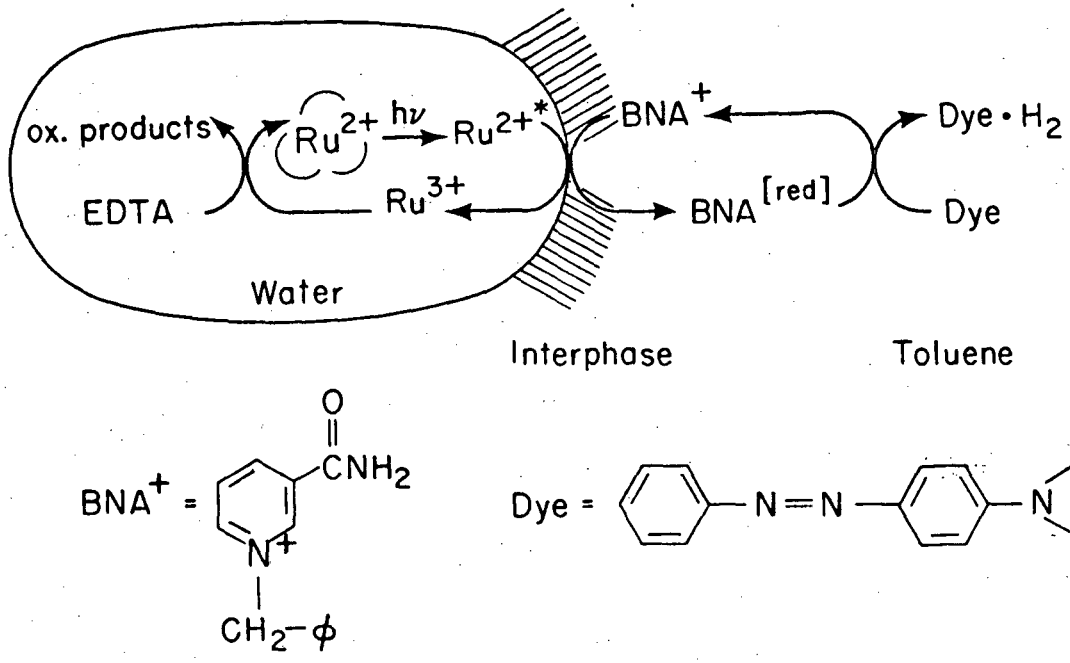

Figure 9

XBL 798-4979

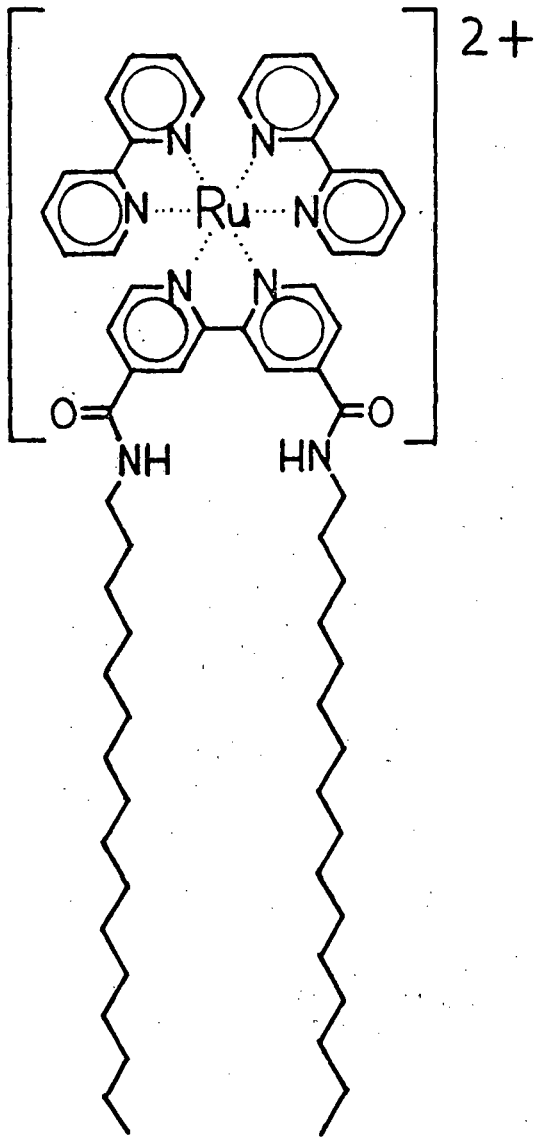

Figure 10

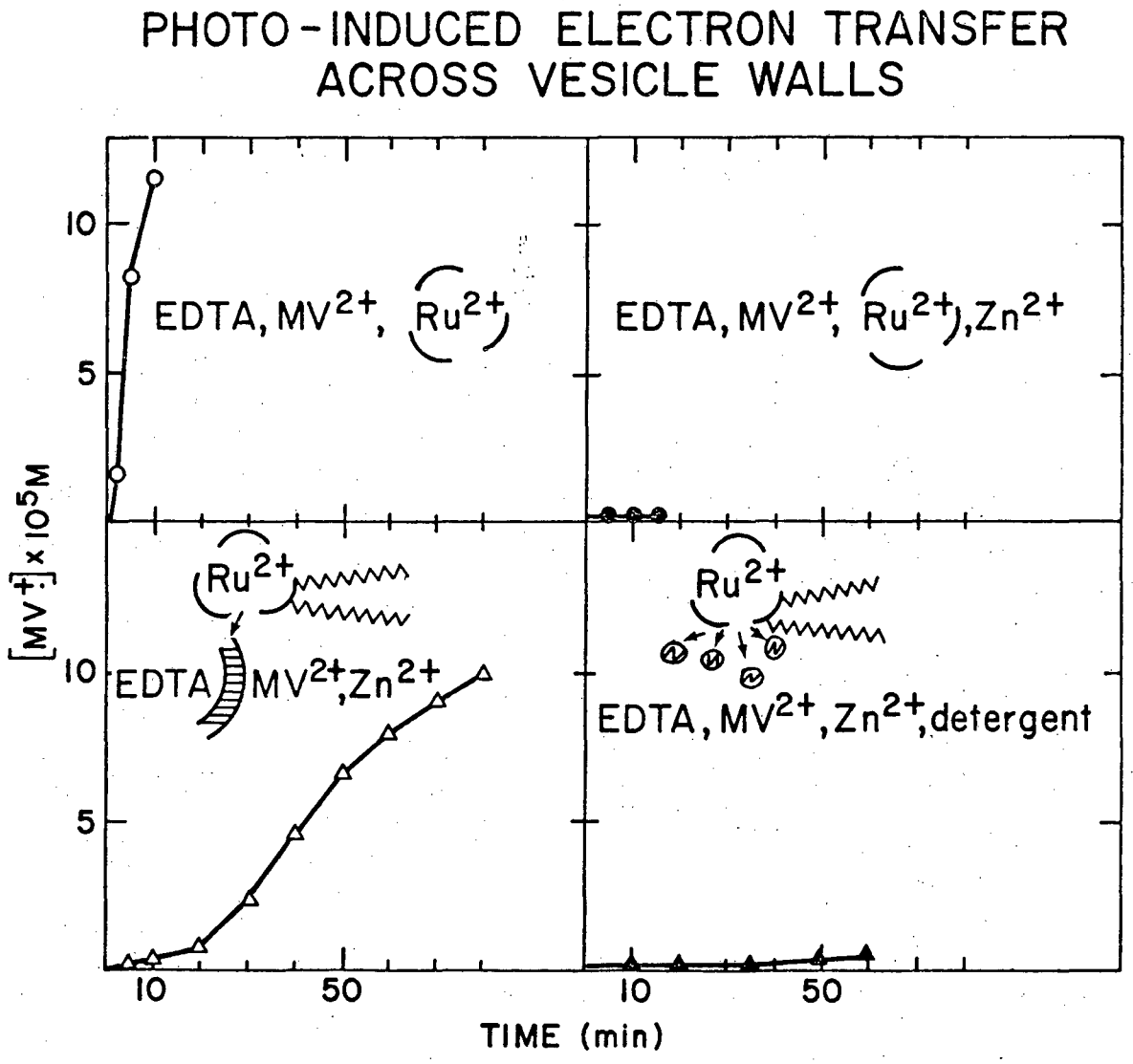
PHOTO-INDUCED ELECTRON TRANSFER
ACROSS VESICLE WALLS
EDTA, MV2+, Ru2+
EDTA, MV2+, Ru2+, Zn2+
Ru2+
EDTA
MV2+, Zn2+
Ru2+
EDTA, MV2+, Zn2+, detergent
[MV+] x 10^5 M
10
5
10
5
10
50
10
50
TIME (min)
XBL 783-3827

Figure 11

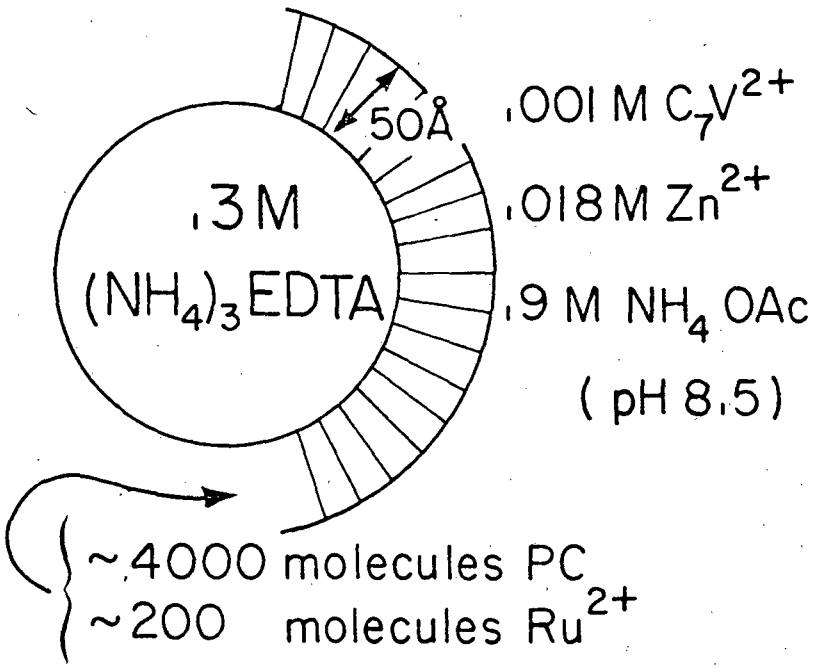

XBL793-4694

Figure 12

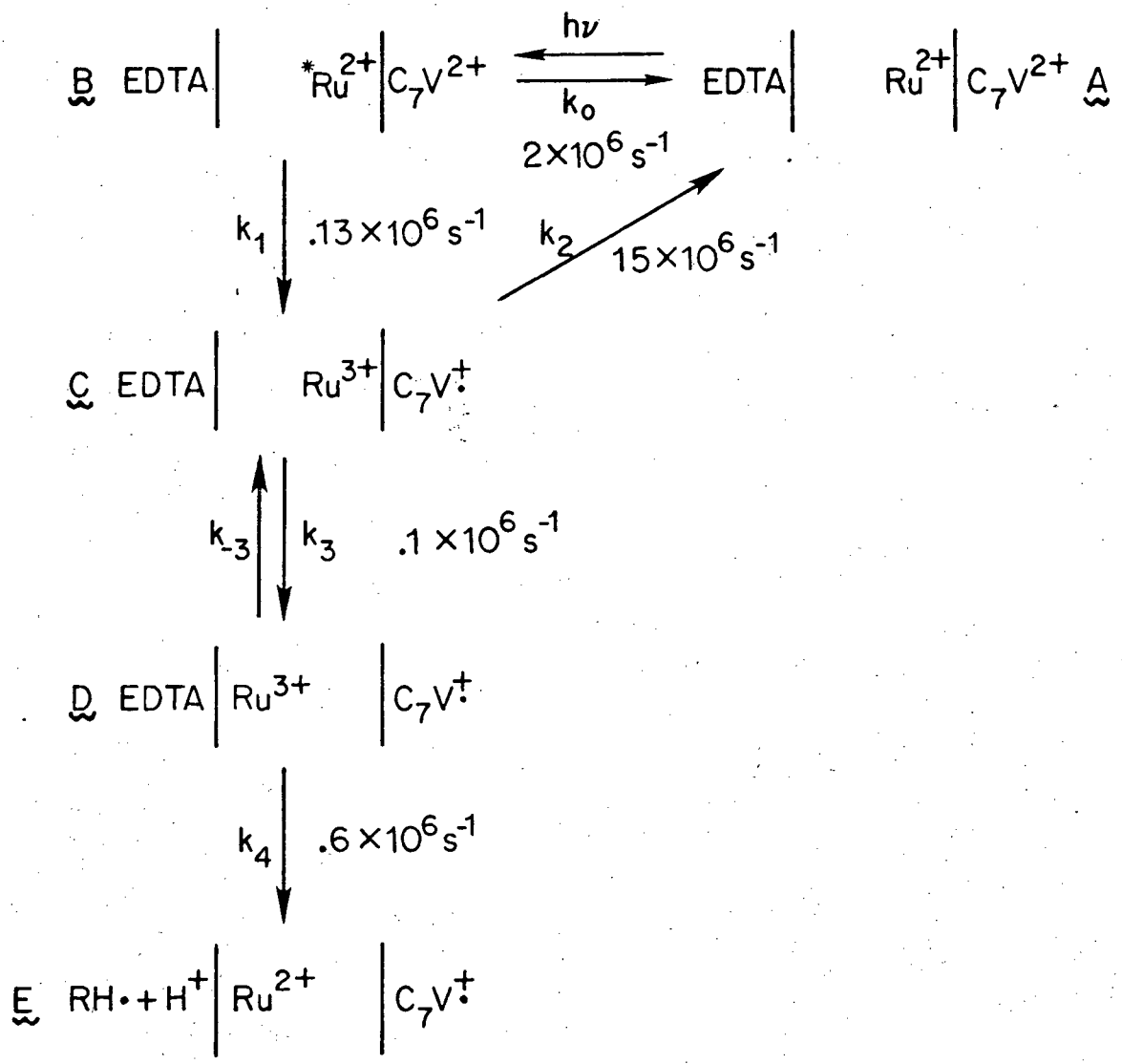

XBL794-4751

Figure 13

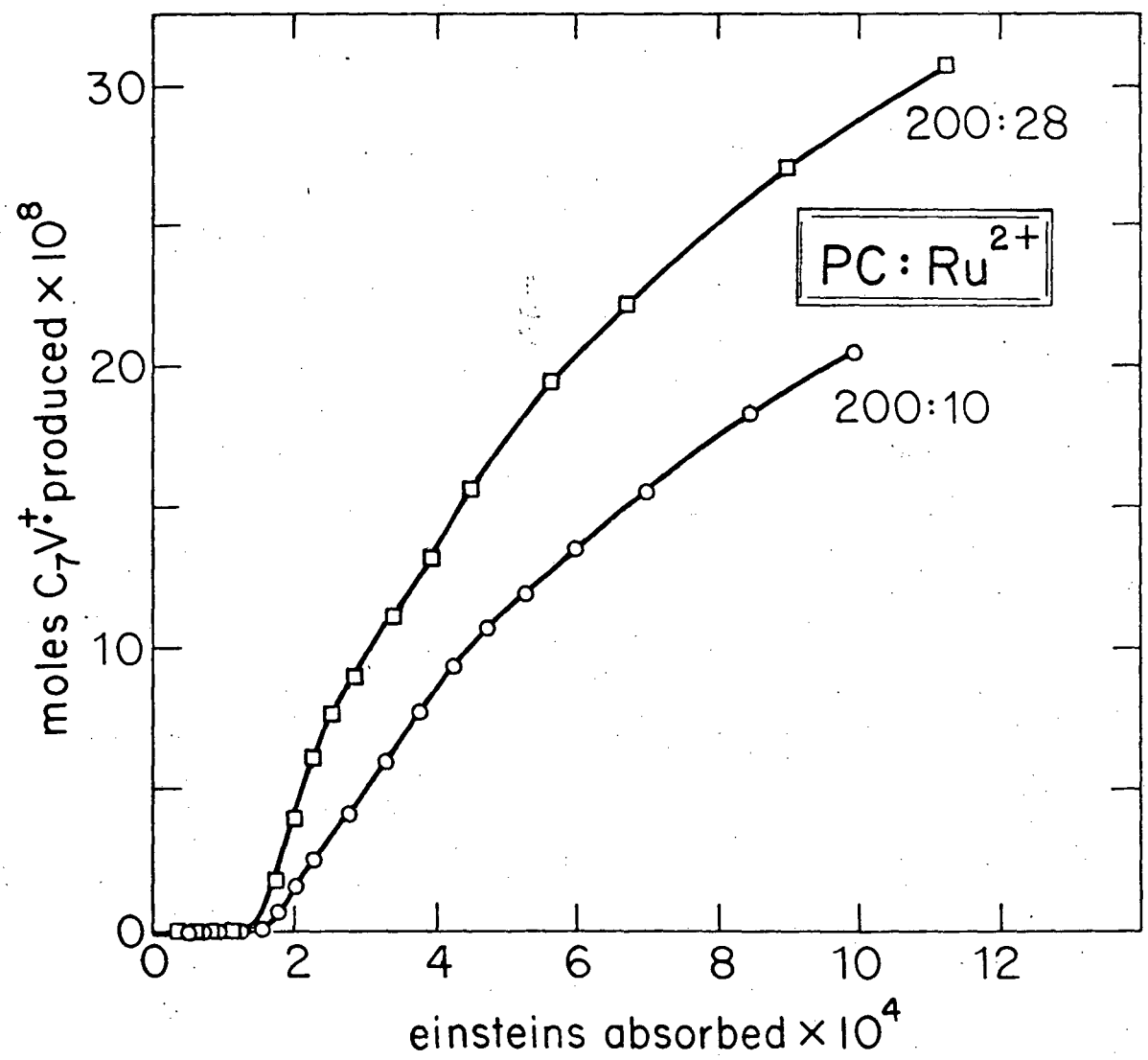
30
20
10
0
0
2
4
6
8
10
12
moles $C_7V^{+\bullet}$ produced $\times 10^8$
einsteins absorbed $\times 10^4$
200:28
200:10
PC : Ru^{2+}
XBL794-4767

Figure 14

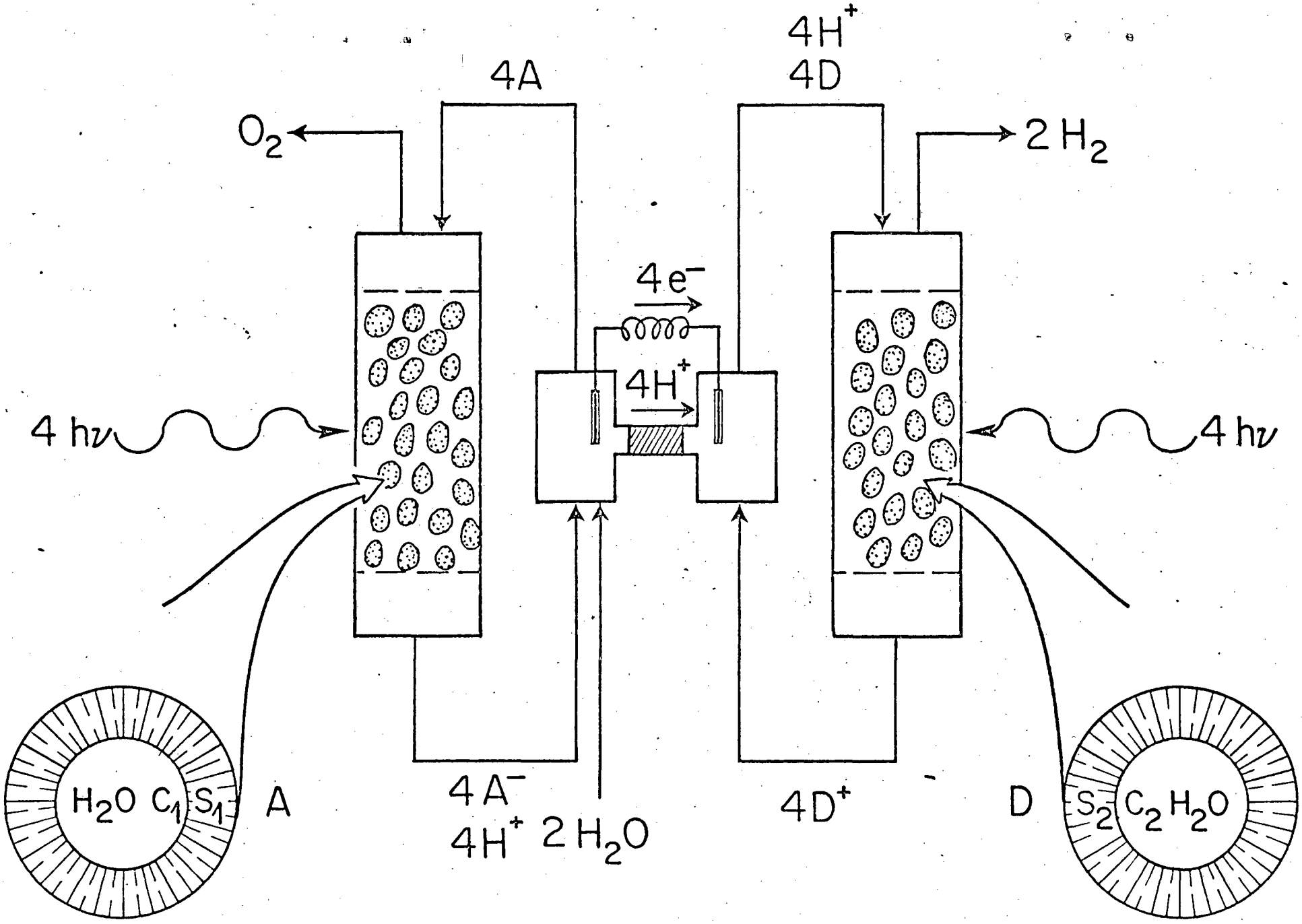

XBL798-498

Figure 15

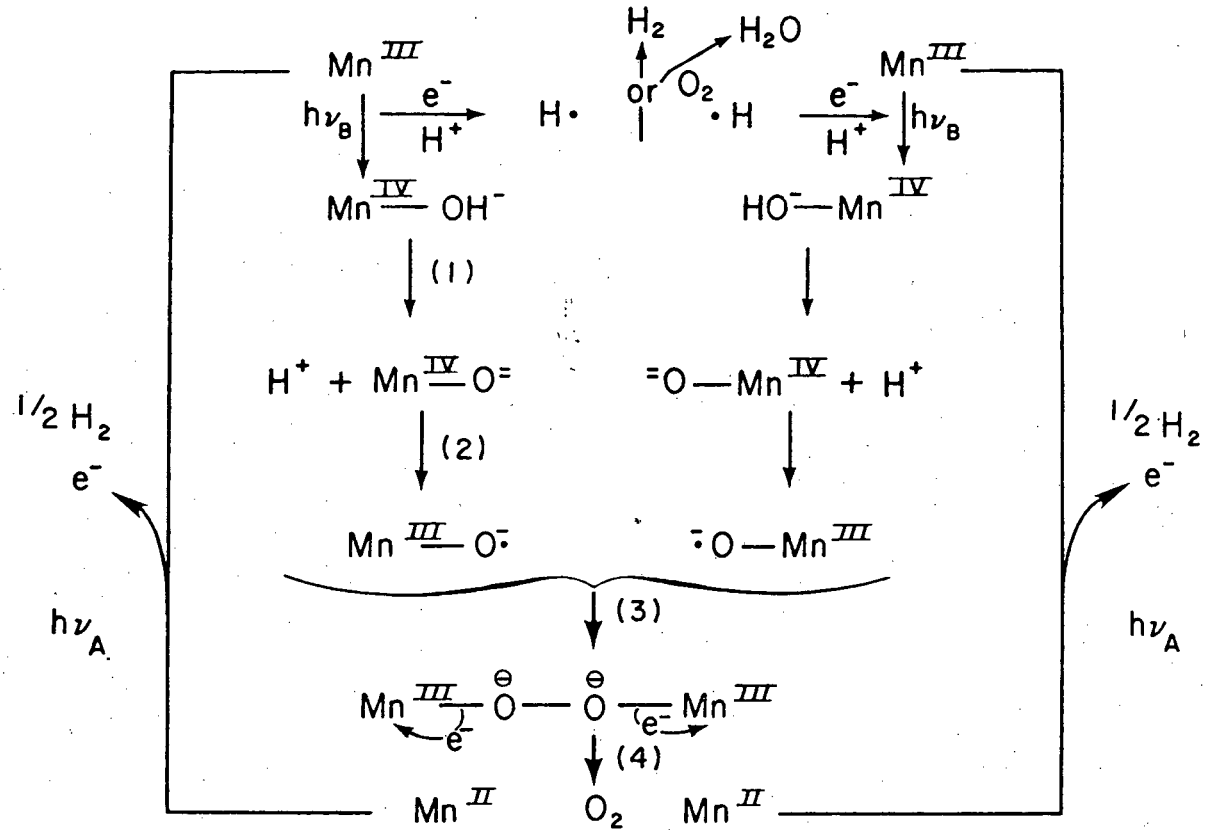

XBL789-4247

Figure 16

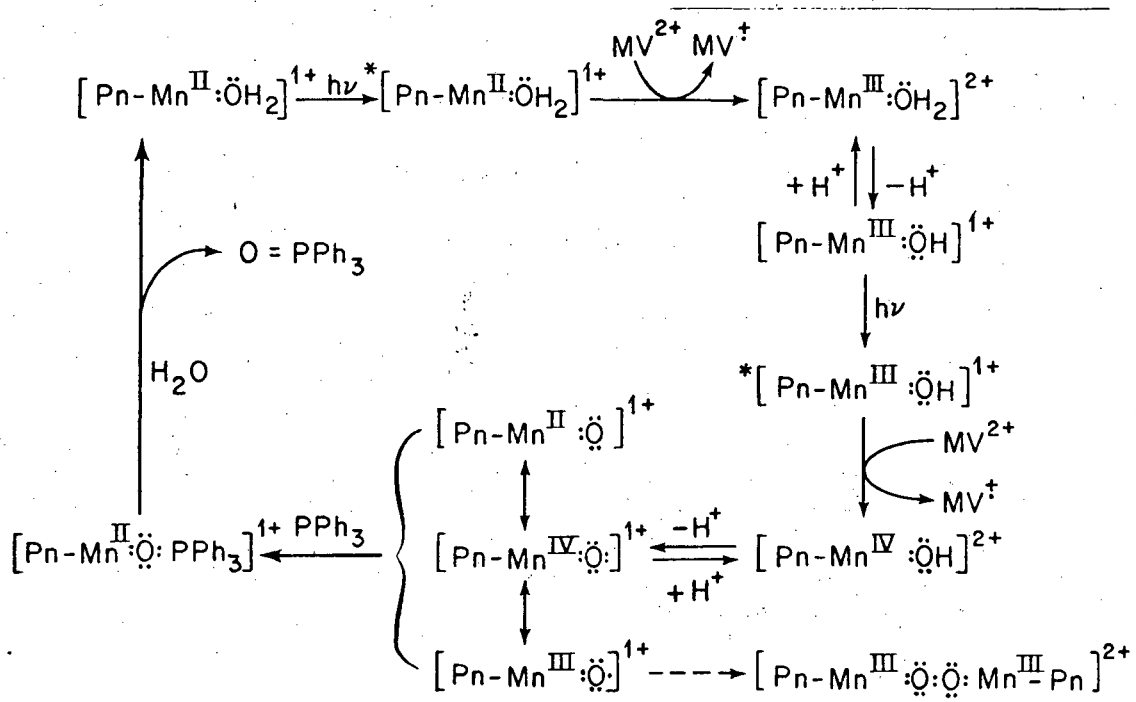

XBL796-4863

Figure 17

TECHNICAL INFORMATION DEPARTMENT
LAWRENCE BERKELEY LABORATORY
UNIVERSITY OF CALIFORNIA
BERKELEY, CALIFORNIA 94720